

Incommensurate correlations in the t - J and frustrated spin- $\frac{1}{2}$ Heisenberg models

Adriana Moreo, Elbio Dagotto, Thierry Jolicoeur,* and José Riera†

Physics Department and Institute for Theoretical Physics, University of California at Santa Barbara, Santa Barbara, California 93106

(Received 18 April 1990)

We analyze the possible existence of incommensurate correlations in the t - J model as a function of doping and in the J_1 - J_2 - J_3 spin- $\frac{1}{2}$ Heisenberg model as a function of frustration using exact diagonalization techniques on small lattices. For the t - J model we found that when holes are introduced the spin structure factor $S(\mathbf{q})$ shifts the position of its maximum away from (π, π) . However, we do not observe indications of the existence of long-range incommensurate order. The frustrated Heisenberg model is analyzed using spin-wave techniques. We present the phase diagram including $1/S$ corrections. It has special regions where there is no magnetic order that are natural candidates for new nonclassical ground states. Using a Lanczos method we study the line $J_3 = J_2/2$, which is completely disordered in the spin-wave analysis for $J_2/J_1 > \frac{1}{4}$. $S(\mathbf{q})$ behaves as in the t - J model replacing doping by frustration. We also study the square of order parameters related with Néel, twisted, dimer, and chiral order. After the Néel order is destabilized by frustration, the twisted and dimer states are enhanced. On the other hand, there are no indications that the uniform or staggered chiral state can be the ground state of the frustrated Heisenberg model.

I. INTRODUCTION

Since the discovery of the new high- T_c superconducting materials¹ there has been a renewal of interest in the theoretical study of strongly correlated electronic systems mainly in two dimensions (2D). Among the most frequently analyzed Hamiltonians are the Hubbard and Heisenberg models with holes (t - J model) and their many variations and generalizations. Many scenarios have been presented where these models lead to a superconducting phase in the presence of doping of holes but none has been universally accepted. Due to the apparent short-range correlations of the new superconductors it is believed that numerical studies may help in deciding what mechanism leads to superconductivity. However, the sign problem of Monte Carlo simulations introduces complications at low temperatures while exact diagonalization studies can handle only small lattices. In this paper we will not address the important (but subtle) issue of the existence of a superconducting phase in the Hubbard model but rather we will concentrate on the possibility of incommensurate correlations in this model at zero temperature ($T=0$) and strong coupling. Understanding the behavior of the ground state of the Hubbard model in different limits may allow us to gain intuition about the superconducting phase (if it exists) and select what approximations and scenarios are more realistic. The importance of a normal-state analysis has been remarked in Ref. 2 where a list of unusual properties of the new materials was presented. Recently, it has been shown numerically³ that one of this abnormal features i.e., the mid-infrared band of the optical conductivity may be explained within the context of the t - J or Hubbard models due to the excitations associated with holes distorting the spin Néel-like background. This is an example of how

important it is to study the strong-coupling limit of Hubbard-like models with some reliable technique like the exact diagonalization method applied to small clusters used in this paper. Features that otherwise seem anomalous or nonstandard may have a clear explanation in these models in a region of parameter space away from weak coupling.

An important feature observed experimentally in the structure factor $S(\mathbf{q})$ of the new materials is an incommensurate double-peaked structure present in superconducting samples which is not present in the nonsuperconducting crystal.⁴ It is not clear in what direction in momentum space that splitting occurs but this situation may be clarified experimentally in the near future. The fact that superconductivity and incommensurability seem to coexist suggest that understanding the splitting of the antiferromagnetic peak with doping may be important in the analysis of the pairing mechanism of the new superconducting materials.

What do we know theoretically about incommensurate phases in strongly correlated electronic systems? Hartree-Fock calculations have been presented for the Hubbard model at large⁵ and small^{6,7} U and for the two-band model.⁸ These studies agree in that there are locally stable solutions of the self-consistent equations consisting of line defects (solitons) in the antiferromagnetic order parameter. While these solutions are not optimal for the magnetic part of the Hamiltonian they provide low-energy modes for the holes which are thus trapped in the solitons. Then, the predictions are that in the Hubbard model at small doping holes form charged lines of defects. For small U they are aligned along the crystal axis⁶ $(0,1),(1,0)$ while for large U along the diagonal⁵ direction $(1,1)$. This effect produces a shift in $S(\mathbf{q})$ similar to that found experimentally. Although these calculations seem

robust it may occur that the Hartree-Fock equations are missing solutions of lower energy and thus an independent calculation without approximations (besides the small size of the system) is important. This is one of the purposes of this paper i.e., we study $S(\mathbf{q})$ in the t - J model (strong-coupling limit of the Hubbard model). Also note that the Coulombic repulsion between holes which is not taken into account in these calculations may destabilize the defects. We will not address this important issue in this paper but in a future work.

While the Hartree-Fock calculations show an incommensurability coming from configurations with spins pointing, for example, in the z direction having a modulation of the amplitude (linearly polarized), a different scenario (recently emphasized by Shraiman and Siggia⁹) may exist. They argued that a mobile hole produces a “roton”-like distortion of the spin background. This distortion is long ranged and decays as $1/r$. In the presence of a finite but small density of holes they found that the commensurate Néel state is unstable at $T=0$ in 2D towards a spiral state where the background spins have incommensurate order characterized by the vector order parameter $\langle \mathbf{S}_i \times \mathbf{S}_{i+\hat{\mathbf{a}}} \rangle$ where \mathbf{S}_i is the spin on site i and $\hat{\mathbf{a}} = \hat{\mathbf{x}}, \hat{\mathbf{y}}$ is a unit vector along the crystal axis. In this phase the spins can be thought of as living on the plane with a small twist (proportional to the hole doping) in some direction.

More exotic spin configurations are also possible. It has been argued in the context of anyonic superconductivity¹⁰ that a uniform order parameter

$$\chi_i = \langle \mathbf{S}_i \cdot (\mathbf{S}_{i+\hat{\mathbf{x}}} \times \mathbf{S}_{i+\hat{\mathbf{y}}}) \rangle$$

which breaks parity (reflexions) and time reversal acquires a nonzero vacuum expectation value. A configuration of spins producing this type of order cannot be accommodated on a plane but it involves the three spatial directions. Although this possibility is very popular among quantum-field theorists, experimental results based on a μ SR (muon spin relaxation)¹¹ as well as numerical studies of frustrated spin- $\frac{1}{2}$ Heisenberg models¹² have shown no evidence of such a spin order. Besides it is not clear if the chiral state will induce a shift in $S(\mathbf{q})$ as found experimentally. There are other even more exotic possibilities: for example Kane *et al.* recently suggested¹³ the existence of a “double-spiral” state where the spins are characterized by a staggered chirality with an order parameter χ_i that changes sign under a translation in one lattice spacing. This staggered, rather than uniform, chiral state was not studied in Ref. 12 and it is another of the purposes of this paper to calculate numerically its value.

There have been some recent previous numerical studies of incommensurability in the Hubbard model with doping.^{14,15} In these quantum Monte Carlo (QMC) simulations a shift in $S(\mathbf{q})$ from (π, π) as a function of doping was observed. No indications were found¹⁴ that in the region of incommensurability there was long-range order since the peaks were not increasing their intensity by increasing the size of the system. Since these results were obtained at nonzero temperature (due to the sign prob-

lem) it is important to check them in an independent calculation at zero temperature.

In addition to the t - J model, in this paper we will also study the related problem of spin systems with frustration. Besides the chiral state described above, many other types of magnetic order have been presented in the literature concerning the frustrated spin- $\frac{1}{2}$ Heisenberg model. For example in a large- N expansion of a generalized Heisenberg model it was concluded¹⁶ that a “dimer” phase (also known as valence bond crystal or spin-Peierls state) may be stable in the Heisenberg model. Another possibility is the existence of a “twisted” state^{17,18} somewhat similar to the spiral phase of the t - J model with holes. Numerically it has been found¹² that both states (dimer and twisted) have chances of being the ground state of the so-called $J_1 - J_2$ model in a narrow region of parameter space. Series expansions¹⁹ seem to favor the presence of dimer order. There are other possibilities in the literature for the ground state of frustrated Heisenberg models like “flux” states²⁰ and resonating valence bond (RVB) states²¹ that we will not discuss in detail here.

The organization of the paper is as follows: In Sec. II we study the spin-spin correlation functions of the t - J model at finite doping. In Sec. III the $J_1 - J_2 - J_3$ frustrated Heisenberg model is analyzed specially for the particular case $J_3 = J_2/2$. Results are presented not only for the spin correlation function but also for different susceptibilities associated with different types of magnetic order. Spin-wave calculations are also discussed. Conclusions are presented in Sec. IV.

II. INCOMMENSURABILITY IN THE t - J MODEL

In this section we concentrate on the t - J model which is defined by the Hamiltonian²²

$$H = J \sum_{i, \hat{\delta}} (\mathbf{S}_i \cdot \mathbf{S}_{i+\hat{\delta}} - \frac{1}{4} n_i n_{i+\hat{\delta}}) - t \sum_{i, \hat{\delta}, \sigma} (\bar{c}_{i, \sigma}^\dagger \bar{c}_{i+\hat{\delta}, \sigma} + \text{H.c.}), \quad (1)$$

where $\bar{c}_{i, \sigma} = c_{i, \sigma} (1 - n_{i, -\sigma})$ is a hole operator acting in the space where there is no double occupancy. $n_{i, \sigma}$ is the number operator ($n_i = \sum_{\sigma} n_{i, \sigma}$), i labels sites of a two-dimensional lattice with periodic boundary conditions and σ is the spin of the electrons. $\hat{\delta}$ connects nearest-neighbors sites. The rest of the notation is standard. The term $-\frac{1}{4} n_i n_{i+\hat{\delta}}$ appears when the t - J is thought of as the strong-coupling limit of the Hubbard model.²³ As numerical technique we use the Lanczos method working on 4×4 lattices due to constraints in the size of the Hilbert space that we can handle numerically. We have studied ground-state properties at all possible doping fractions in this lattice which is a considerable larger numerical effort with respect to previous studies that have concentrated only on the 0, 1 and 2 holes subspaces. For example, on the 4×4 lattice the subspace with the maximum size corresponds to 5 and 6 holes and total spin projection $S_z = \frac{1}{2}$ and 0, respectively, with a total number of states of 2 018 016 (reduced in practice by symmetries).

This is ~ 5 (~ 157) times bigger than the subspace of 2 holes (0 holes) with $S_z=0$. A Cray-2 supercomputer which has a large memory was necessary for the present study. Typical accuracy of energies in the ground state was of 10^{-9} .

In Fig. 1 we present the ground-state mean value of the spin-spin correlation function in momentum space

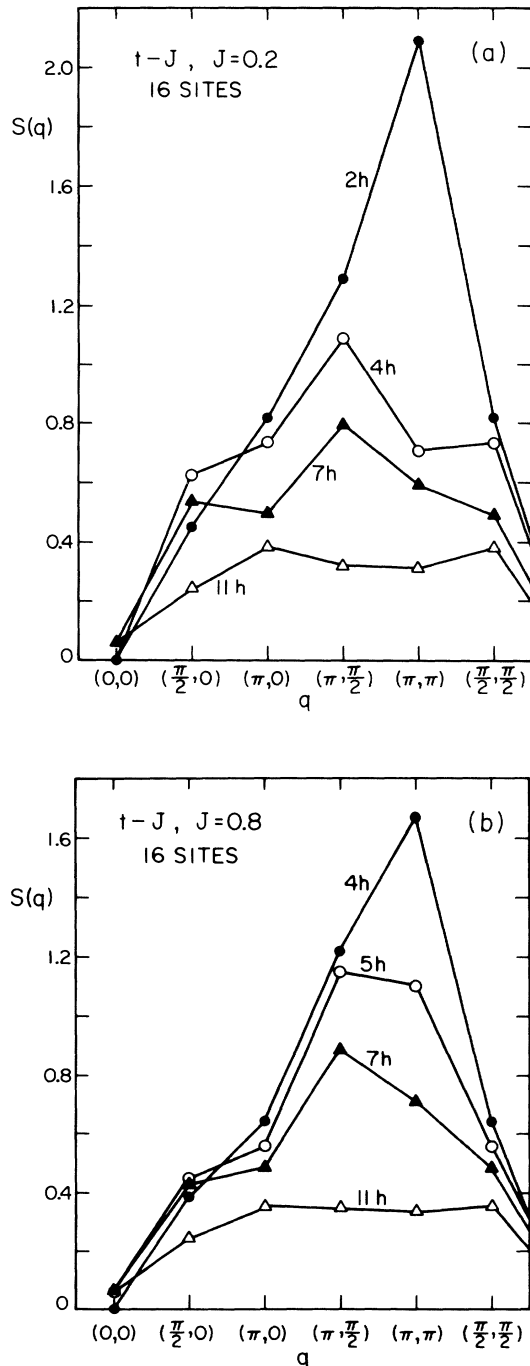


FIG. 1. (a) Spin-spin correlation function $S(\mathbf{q})$ as a function of momentum for the 4×4 lattice and different number of holes. $J=0.2, t=1$. (b) Same as Fig. 1(a) but for $J=0.8$.

defined as

$$S(\mathbf{q}) = \frac{1}{\sqrt{N}} \sum_{\mathbf{l}, \mathbf{j}} e^{i(\mathbf{l}-\mathbf{j}) \cdot \mathbf{q}} \langle \psi_{\text{gs}}^{nh} | S_{\mathbf{l}}^z S_{\mathbf{j}}^z | \psi_{\text{gs}}^{nh} \rangle, \quad (2)$$

where $|\psi_{\text{gs}}^{nh}\rangle$ is the ground state of the system in the subspace with nh holes and N the number of sites. The sum in \mathbf{l}, \mathbf{j} is over all the sites of the lattice. In Fig. 1(a) it can be observed that for $J=0.2$ and two holes ($nh=2$) the maximum in $S(\mathbf{q})$ is still at $\mathbf{q}=(\pi, \pi)$ as it happens at half-filling, but with a reduced intensity since for this lattice $S(\pi, \pi) \sim 5.9$ in the case of zero holes. The important detail is that with four holes the maximum is obtained at the next available momentum on our 4×4 lattice which is $\mathbf{q}=(\pi, \pi/2)$ rather than at (π, π) . The intensity of the peak is greatly reduced with respect to the $\mathbf{q}=(\pi, \pi)$ peak at lower doping. Increasing the number of holes up to 11 holes we observe that $S(\mathbf{q})$ is now virtually flat obtaining its maximum value at $(0, \pi)$ and $(\pi/2, \pi/2)$ which are degenerate on the 4×4 lattice.²⁴ A very similar situation is observed in Fig. 1(b) at $J=0.8$. In this case the peak is at $\mathbf{q}=(\pi, \pi)$ even for 4 holes i.e., more doping is required to start moving the antiferromagnetic (AF) peak than at small J .

Our results indicate that as a function of doping the t - J model has a tendency to develop incommensurate correlations between the spins. This is a nontrivial result since the peak at (π, π) could have simply reduced its intensity with doping without changing its position. Our results are in qualitative agreement with experiments⁴ and also with the frustrated Heisenberg model results described in the next section. However, note that studying only one lattice size we cannot show whether the peaks at momentum different from (π, π) will diverge in the thermodynamic limit. The intensity of the shifted peaks is very much suppressed with respect to the case of (π, π) at half-filling and that may be an indication that the correlations will remain of short range in the bulk limit although only a study in larger lattices will clarify the situation. In Fig. 2 we show the “phase diagram” of the t - J model obtained by monitoring the position of the maximum in

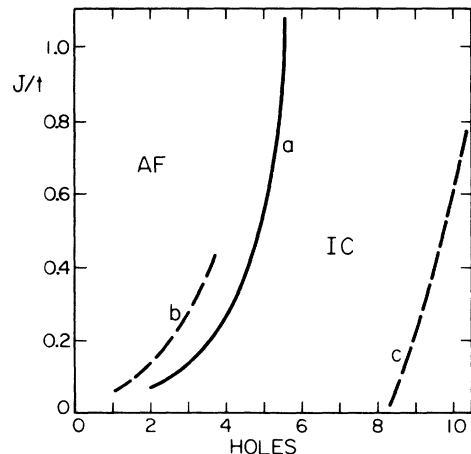


FIG. 2. “Phase diagram” of the t - J model showing the regions where the maximum in the spin-spin correlation is at (π, π) (AF) or at $(\pi, \pi/2)$ (IC). For more details see the text.

$S(\mathbf{q})$. The AF region indicates that the maximum is at (π, π) while incommensurate (IC) denotes that the maximum is now at $(\pi, \pi/2)$ (they are separated by line a). For large J/t more doping is needed than at small J/t to move the AF peak. This may be due to the fact that antiferromagnetic correlations are more robust for almost static holes than for highly mobile ones. For very small J/t it is difficult to decide if the line separating the AF and IC region will move smoothly to zero doping as $J/t \rightarrow 0$. This difficulty comes from many sources: (i) on a 4×4 lattice the finite-size effects at small J/t and low doping are important for $J/t < 0.1$ as was recently²⁴ shown, (ii) in that regime ferromagnetic instabilities are important. Actually in Fig. 2 we found, although we did not show it there, a ferromagnetic phase at very small J/t and intermediate doping. We have also not analyzed in detailed the possibility of phase separation in this model,²⁵ only the IC correlations. Finally, line c is a crossover to a regime where the spin-spin correlation function is virtually flat.

It is clear that using a 4×4 lattice we have very little resolution to analyze at what doping the antiferromagnetic peak begins moving from (π, π) . One way to improve on this situation is to use twisted boundary conditions which allow momenta different from those of a lattice with periodic boundary conditions. For that purpose we can define at the boundary an angle θ and a new boundary condition BC given by²⁶ $\bar{c}_{(L_x+1, i_y), \sigma} = e^{i\theta} \bar{c}_{(1, i_y), \sigma}$, where L_x is the length of the lattice in the direction x , $\mathbf{i} = (i_x, i_y)$ and a similar definition holds for the direction y . The Hamiltonian can be diagonalized numerically with this boundary condition and $S(\mathbf{q})$ can be studied as a function of θ . Since this is very computer time consuming, in this paper we have only studied the special case of antiperiodic boundary conditions (ABC) in both directions which produce momenta $q_x = (2\pi/L)(n_x + \frac{1}{2})$ and $q_y = (2\pi/L)(n_y + \frac{1}{2})$ on a $L \times L$ lattice ($n_x, n_y = 0, \dots, L-1$). Line b in Fig. 2 shows the results obtained with ABC and small J/t for the line separating the AF and IC regions. With this BC the line where the antiferromagnetic peak starts moving occurs at smaller doping than with PBC. This is obvious since now we have an additional momentum between (π, π) and $(\pi, \pi/2)$. Without a more detailed study we can not show for a given J at what value of the doping the AF peak starts moving. However, Fig. 2 seems to suggest that the movement of the (π, π) peak does *not* begin immediately with doping. To show this we assume that the position of the maximum is given by $\mathbf{Q} = (\pi, \pi) - a\delta(1, 0)$ where δ represents doping and a is a constant. Since with PBC the closest momentum to (π, π) is $(\pi/2, \pi)$ while for ABC it is $(3\pi/4, 3\pi/4)$, it is (roughly) true that the “critical” dopings of each BC for a given J should differ by a factor ~ 2 . This behavior is not clear from Fig. 2. For example, at $J=0.4$ the point where the IC “phase” starts in the bulk limit is better approximated by $\delta_c \sim 2.5$ (linear extrapolation) than by 0. If this result is confirmed, then it will have important implications for theories of superconductivity based on spin bags²⁷ since these polarons will be stable in a finite doping region near half-filling.

In Fig. 3 we show the AF and IC spin structure factors versus doping. From this figure it is clear that the incommensurate correlations are actually not much enhanced with doping but rather the AF ones are very much *suppressed*. There is no evidence that the IC form factor will diverge in the bulk limit. This is also in agreement with the QMC results of Moreo *et al.*¹⁴ for the Hubbard model. We think that this type of behavior may well be a common feature of many strongly correlated electronic systems. Note also that in our study on a 4×4 lattice we cannot distinguish if the maximum in $S(\mathbf{q})$ migrates with doping towards $(0, \pi)$, $(\pi, 0)$ or along the diagonal in momentum space.

There are mean-field studies of the t - J model to compare our results with. For example, Jayaprakash *et al.*²⁸ also found a “spiral” (IC) phase in the t - J model producing a phase diagram qualitatively very similar to our Fig. 2. The differences with our results are the following. (i) the actual position of the different phases. Their ferromagnetic phase is too much enhanced, (ii) the spiral phase at small J/t appears as soon as doping is turn on in the mean-field calculation. This may be a problem of this approximation or a lack of resolution of our small lattice to obtain correctly the “critical” doping where the AF peak starts moving. Other differences are that these mean-field calculations^{28,13} predict *long-range* incommensurate correlations along the diagonal (1,1) for the t - J model. We only have observed evidence of *short-range* IC correlations. Also note that the QMC results¹⁴ show movement of the peaks along (0,1),(1,0) rather than (1,1) but that occurs in the small U Hubbard model and the situation can be different at large U . In any case, it is very encouraging that both an analytic mean-field calculation and a numerical study agree in the existence of IC correlations in this type of models. More detailed results with ground-state energies at various fillings, analysis of binding of holes and susceptibilities of different order parameters will be presented in a future publication.

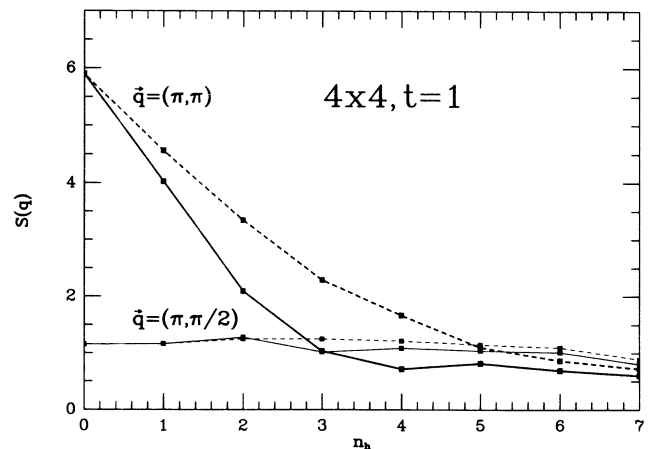


FIG. 3. $S(\mathbf{q})$ as a function of the number of holes. The thick continuous (dashed) line denotes $\mathbf{q} = (\pi, \pi)$ and $J=0.2$ ($J=0.8$); while the thin continuous (dashed) line indicates $\mathbf{q} = (\pi, \pi/2)$ and $J=0.2$ ($J=0.8$).

III. INCOMMENSURABILITY IN THE $J_1 - J_2 - J_3$ MODEL

In this section we study the frustrated spin- $\frac{1}{2}$ Heisenberg model defined as

$$H = J_1(H_1 + \alpha_2 H_2 + \alpha_3 H_3) \\ = J_1 \sum_{i, \delta_1} \mathbf{S}_i \cdot \mathbf{S}_{i+\delta_1} + J_2 \sum_{i, \delta_2} \mathbf{S}_i \cdot \mathbf{S}_{i+\delta_2} + J_3 \sum_{i, \delta_3} \mathbf{S}_i \cdot \mathbf{S}_{i+\delta_3}, \quad (3)$$

where \mathbf{S}_i is a spin- $\frac{1}{2}$ variables at site $i = (i_x, i_y)$ of a square lattice with PBC. δ_1 connects sites of the lattice at distance 1, δ_2 at distance $\sqrt{2}$ (along the diagonals of the plaquettes of the lattice), δ_3 at distance 2 and $\alpha_{2,3} = J_{2,3}/J_1$. The study of this Hamiltonian is interesting per se since not much is known about ground-state properties of frustrated models when quantum fluctuations are taken into account in two dimensions. As a further motivation for this analysis, it has been conjectured²⁹ that a relation may exist between the Hubbard or t - J models with doping and the $J_1 - J_2 - J_3$ model Eq. (3) for the particular case of $J_3 = J_2/2$. In this framework the spin couplings are functions of U, t and doping δ of the Hubbard model.

The special case of $J_3 = 0$ was previously studied using exact diagonalization techniques¹² on lattices of 16 and 20 sites. The main conclusions of that analysis were that: (i) for large J_2 the rotational symmetry of the lattice is spontaneously broken due to the phenomenon of "order from disorder" in which a degenerate classical ground state lifts its degeneracy by quantum fluctuations^{30,18} (we will describe this calculation in detail in the appendix), (ii) in the region near $J_2/J_1 \sim 0.5$ where chances are that quantum effects may lead to a new ground state³¹ we found that the dimer¹⁶ and twisted states¹⁷ have a peak in the square of their order parameters suggesting that one of them (or both in some combination) may be stable in a narrow region of parameter space. This result should be contrasted with those of series expansion calculations¹⁹ where it was found that the dimer state was stable in the $J_1 - J_2$ model (also in a narrow region near $J_2/J_1 \sim 0.5$) while the twisted state was not enhanced.³² Numerical results in larger lattices (in progress) will clarify this issue. The order parameter of the uniform chiral state was found to be featureless and thus there were no indications that such a state was the ground state. Below, first we discuss spin-wave results for this model and then elaborate on the numerical results along the line $J_3 = J_2/2$.

A. Spin-waves calculation

In this subsection we present results based on the standard spin-wave formalism applied to the $J_1 - J_2 - J_3$ model. We include many details of the calculation to make the section self-consistent for nonexperts in this subfield. As usual we use the Holstein-Primakov method where the SU(2) algebra of the spin operators is realized through the use of a set of bosonic harmonic oscillators, the so-called Holstein-Primakov (HP) bosons:

$$S_i^z = S - b_i^\dagger b_i, \\ S_i^+ = \sqrt{2S - b_i^\dagger b_i} b_i, \\ S_i^- = b_i^\dagger \sqrt{2S - b_i^\dagger b_i}, \quad (4)$$

with the standard commutation relation: $[b_i, b_j^\dagger] = \delta_{ij}$. We use this parametrization of the quantum spins to study fluctuations around a classical ground state. The expansion parameter is then $1/S$. Of course, one can at best hope to obtain qualitative results when setting S equal to $\frac{1}{2}$. However, in the unfrustrated case there is some evidence that the semiclassical approximation captures the essential physics. So it can be an interesting guide to our *ab initio* Lanczos study.

We will describe the calculation in the Néel phase and present results for the rest of the phase diagram. Let us study what happens in the case of small J_2 and J_3 . When $J_3/J_1 \leq \frac{1}{4} - \frac{1}{2}J_2/J_1$ the classical ground state has the conventional Néel order with two sublattices and it is non degenerate (the degeneracy due to rotational invariance is spontaneously broken). As explained in textbooks³³ it is convenient to reflect the x and z axis (for example) in one sublattice in order to consider fluctuations about the Néel state. After this reflection, for the nearest neighbors (NN) part of the Hamiltonian we write

$$H_1 = \sum_{\text{NN}} \mathbf{S}_i \cdot \mathbf{S}_j = \sum_{\text{NN}} [-(S_i^x S_j^x + S_i^z S_j^z) + S_i^y S_j^y], \quad (5)$$

while for the couplings at distance 2 and $\sqrt{2}$ there is no $(-)$ sign since the sublattices are ordered in a ferromagnetic way. Using the HP representation, expanding the square roots and keeping only the terms which are quadratic in the b, b^\dagger operators we obtain the first nontrivial order in the semiclassical approximation. For H_1 , one finds

$$H_1 = -S^2 2N + S \sum_{\text{NN}} (b_i^\dagger b_i + b_j^\dagger b_j - b_i b_j - b_i^\dagger b_j^\dagger), \quad (6)$$

where N is the number of sites on a square lattice. By Fourier transforming, this can be written as

$$H_1 = -S^2 2N + 4S \sum_{\mathbf{k}} [b_{\mathbf{k}}^\dagger b_{\mathbf{k}} - \frac{1}{2} \gamma_{\mathbf{k}} (b_{\mathbf{k}} b_{-\mathbf{k}} + b_{\mathbf{k}}^\dagger b_{-\mathbf{k}}^\dagger)], \quad (7)$$

where the sum over \mathbf{k} runs over the first Brillouin zone $[-\pi, \pi]^2$ of a two-dimensional lattice and

$$\gamma_{\mathbf{k}} = \frac{1}{2} [\cos(k_x) + \cos(k_y)].$$

We perform the same treatment on H_2

$$H_2 = \alpha_2 S^2 2N + \alpha_2 S \sum_{\text{NNN}} (b_i^\dagger b_j + b_j^\dagger b_i - b_i^\dagger b_i - b_j^\dagger b_j), \quad (8)$$

which in momentum space is

$$H_2 = \alpha_2 S^2 2N - 4\alpha_2 S \sum_{\mathbf{k}} (1 - \gamma'_{\mathbf{k}}) b_{\mathbf{k}}^\dagger b_{\mathbf{k}}, \quad (9)$$

where $\gamma'_{\mathbf{k}} = \cos(k_x) \cos(k_y)$. The result for H_3 is obtained from Eq. (9) for H_2 by replacing $\alpha_2 \rightarrow \alpha_3$ and

$$\gamma_{\mathbf{k}} \rightarrow \gamma''_{\mathbf{k}} = \frac{1}{2} [\cos(2k_x) + \cos(2k_y)].$$

We thus have to diagonalize the following quadratic form in the HP bosons:

$$4S \sum_{\mathbf{k}} \{ [1 - \alpha_2(1 - \gamma'_k) - \alpha_3(1 - \gamma''_k)] \times b_{\mathbf{k}}^\dagger b_{\mathbf{k}} - \frac{1}{2} \gamma_k (b_{\mathbf{k}} b_{-\mathbf{k}} + b_{\mathbf{k}}^\dagger b_{-\mathbf{k}}^\dagger) \}. \quad (10)$$

This can be done by using a Bogoliubov transformation

$$b_{\mathbf{k}} = \alpha_{\mathbf{k}} \cosh \theta_{\mathbf{k}} + \alpha_{-\mathbf{k}}^\dagger \sinh \theta_{\mathbf{k}}, \quad \tanh(2\theta_{\mathbf{k}}) = \frac{\gamma_{\mathbf{k}}}{[1 - \alpha_2(1 - \gamma'_k) - \alpha_3(1 - \gamma''_k)]}. \quad (11)$$

At this order in $1/S$ we obtain a Hamiltonian describing decoupled spin waves

$$4S \sum_{\mathbf{k}} [1 - \alpha_2(1 - \gamma'_k) - \alpha_3(1 - \gamma''_k)] \times \left[\frac{1}{\cosh(2\theta_{\mathbf{k}})} (\alpha_{\mathbf{k}}^\dagger \alpha_{\mathbf{k}} + \frac{1}{2}) - \frac{1}{2} \right]. \quad (12)$$

Higher-order terms will lead to interactions between these modes. The zero-point motion of the harmonic oscillators $\alpha_{\mathbf{k}}$ produces a shift of the energy with respect to its classical value and also decreases the mean value in the ground state of S^z , the sublattice magnetization. Since the vacuum is at this order defined by $\alpha_{\mathbf{k}}|O\rangle = 0$, one finds that the staggered magnetization $\langle S^z \rangle = S - \langle b^\dagger b \rangle$, is

$$\langle S^z \rangle = S + \frac{1}{2} - \frac{1}{2N} \sum_{\mathbf{k}} \frac{1}{[1 - \tanh(2\theta_{\mathbf{k}})]^{1/2}}. \quad (13)$$

Taking $\alpha_3 = 0$ in Eq. (13) it can be found³¹ that $\langle S^z \rangle$ vanishes somewhere before $\alpha_2 = \frac{1}{2}$ when the spin S is set to the value $\frac{1}{2}$. For $S = \frac{1}{2}$ and $\alpha_2, \alpha_3 = 0$ we obtain $\langle S^z \rangle \approx 0.30$ showing the reduction of 60% in the classical magnetization due to quantum fluctuations. Independent of the value of S , Eqs. (12) and (13) become singular at the classical limiting point $J_3/J_1 = \frac{1}{4} - \frac{1}{2} J_2/J_1$. This is due to the fact that beyond this point the classical ground state is no longer the Néel state. For the ground-state energy, we find

$$\frac{E_0}{NJ_1} = -2S(S+1)(1 - \alpha_2 - \alpha_3) + 2S \int \frac{d^2k}{(2\pi)^2} \{ [1 - \alpha_2(1 - \gamma'_k) - \alpha_3(1 - \gamma''_k)]^2 - \gamma_k^2 \}^{1/2}. \quad (14)$$

From Eq. (13) we can obtain the boundary of the Néel phase with $S = \frac{1}{2}$ as the point where $\langle S^z \rangle$ vanishes. Numerically studying this equation we found that this boundary is approximately given by the straightline $J_3/J_1 \approx 0.2 - 0.5J_2/J_1$. This is shown explicitly in Fig. 4 where we also present the rest of the phase diagram. At $S = \frac{1}{2}$ there are four distinct ordered phases separated by a narrow disordered region. Phase 1 is the Néel phase already discussed, phase 2 corresponds to a phase which is infinitely degenerate at the classical limit. The quantum

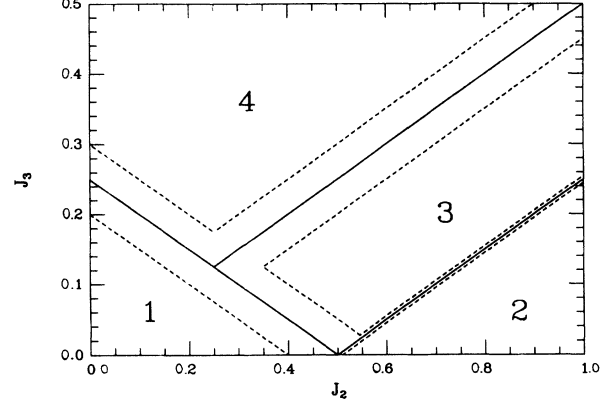


FIG. 4. Phase diagram of the J_1 - J_2 - J_3 model from a spin-wave calculation to order $1/S$. The meaning of the different phases and lines of transitions is explained in the text.

fluctuations drastically affect this degeneracy as discussed in the appendix producing a spontaneous breaking of rotational invariance.¹² Phase 3 corresponds to an incommensurate phase ordered with momentum $(\pi, \pm Q), (\pm Q, \pi)$ where $\cos(Q) = (2J_2 - J_1)/4J_3$ while phase 4 is also an IC phase with momentum $(\pm Q, \pm Q)$ where $\cos(Q) = -J_1/(2J_2 + 4J_3)$. The continuous lines in Fig. 4 denote the boundaries between the different phases in the classical limit and the dashed lines are the borders of the disordered regions found in the spin-wave approximation.³⁴

Note that the line $J_3 = J_2/2$ is very particular.³⁵ At the classical level and for $\alpha_2 > \frac{1}{4}$ it corresponds to a line of phase transitions between two IC regions. It has an infinite degeneracy of spiral states given by

$$\cos(Q_x) + \cos(Q_y) = -\frac{1}{2\alpha_2}, \quad (15)$$

but quantum fluctuations completely disorder this line (Fig. 4). It is thus a natural candidate for the search of a new nonclassical ground state in the frustrated Heisenberg model and we will study it in detail in the next subsection.

For completeness we present here some general results valid for all the phases of Fig. 4. We have performed the SW expansion about a ground state with a spiral state characterized by wave vector Q_0 . This vector Q_0 has to minimize the function $J(\mathbf{k})$ where

$$J(\mathbf{k}) = \frac{1}{2} [\cos(k_x) + \cos(k_y)] + J_2 \cos(k_x) \cos(k_y) + (J_3/2) [\cos(2k_x) + \cos(2k_y)]. \quad (16)$$

The ground-state energy is then (setting $S = \frac{1}{2}$)

$$\frac{E_0}{NJ_1} = \frac{3}{2} J(Q_0) + \frac{\sqrt{2}}{8\pi^2} \int d^2k \{ [J(\mathbf{k}) - J(Q_0)] \times [J(Q_0 + \mathbf{k}) + J(Q_0 - \mathbf{k}) - 2J(Q_0)] \}^{1/2}. \quad (17)$$

The staggered magnetization is given by

$$\langle S^z \rangle = S + \frac{1}{2} - \frac{1}{2N} \sum_{\mathbf{k}} [1 - \tanh^2(2\theta_{\mathbf{k}})]^{-1/2}, \quad (18)$$

where

$$\tanh(2\theta_{\mathbf{k}}) = \frac{-B_{\mathbf{k}}}{[B_{\mathbf{k}} + J(\mathbf{k}) - J(Q_0)]} \quad (19)$$

and

$$B_{\mathbf{k}} = \frac{1}{4}[J(Q_0 + \mathbf{k}) + J(Q_0 - \mathbf{k})] - \frac{1}{2}J(\mathbf{k}). \quad (20)$$

B. Lanczos results

In this subsection we present the Lanczos results for the J_1 - J_2 - J_3 model in the special limit of $J_3 = J_2/2$. We used square lattices of 16 and 20 sites with PBC identical to those analyzed in our previous study of the J_1 - J_2 model.^{12,36} We study the ground-state energy and quantum numbers as well as mean values of selected operators. Typical accuracy in the ground-state energies of our study is 10^{-9} .

In Fig. 5(a) we show the ground-state energy per site for a 4×4 lattice at $J_1 = 2.0$ and other selected levels corresponding to states with the lowest energy in different subspaces [there are other levels above and in between those shown in Fig. 5(a)]. The ground state E^+ is a spin singlet with zero momentum $\mathbf{k} = (0,0)$, even under a rotation of the lattice in $\pi/2$ and even under a reflexion with respect to some axis. E^- differs from the ground state only in the quantum number under rotations in $\pi/2$ since this state is odd under that operation. E_{SW1} denotes the lowest-energy state with momentum $\mathbf{k} = (\pi, \pi)$ and spin one (spin wave), E_{SW2} is also a spin one state but with $\mathbf{k} = (\pi, 0)$ or $(0, \pi)$ while E_{SW3} has spin one and momentum $(\pi, \pi/2)$ or it is rotated.

In Fig. 5(b) we show a similar result but for the 20 site lattice with the same meaning for the different levels. A difference to remark with respect to Fig. 5(a) is that with $N=20$ and at $J_2 \sim 2.0$ there is a crossing of levels between the E^+ and E^- states. The same occurred in the J_1 - J_2 model¹² and perhaps it is a finite-size effect. In this figure we also present the energy of the ground state in the spin-wave approximation described before (dashed line) for $1/S=2$. Both qualitatively and quantitatively it is an excellent approximation to the actual ground-state energy. Even beyond the point where long-range order is lost in this method, the predicted energy lies very close to its correct value (this shows us that the region where the energy is maximum is not necessarily related with a critical region). Finally note that although in Fig. 5(b) we do not show other spin-wave states rather than $E_{SW1,2}$, they may have a small energy in the intermediate region.

In Fig. 6 we show the square of the staggered magnetization defined as

$$M^2 = \left\langle 3 \left[\frac{1}{N} \sum_{\mathbf{i}} (-1)^{i_x + i_y} S_{\mathbf{i}}^z \right]^2 \right\rangle, \quad (21)$$

as a function of J_2 (at $J_1 = 2$ and $J_3 = J_2/2$). As expected, in the absence of frustration ($J_2 = 0$) this correlation

function has a large value corresponding to a Néel state but when frustration is turned on it quickly decreases. From Fig. 6 it is difficult to say at what critical coupling it will vanish. However, note that around $J_2 \sim 0.7$, M^2 changes concavity which may be due to our study of the square of the order parameter. Then, a reasonable guess

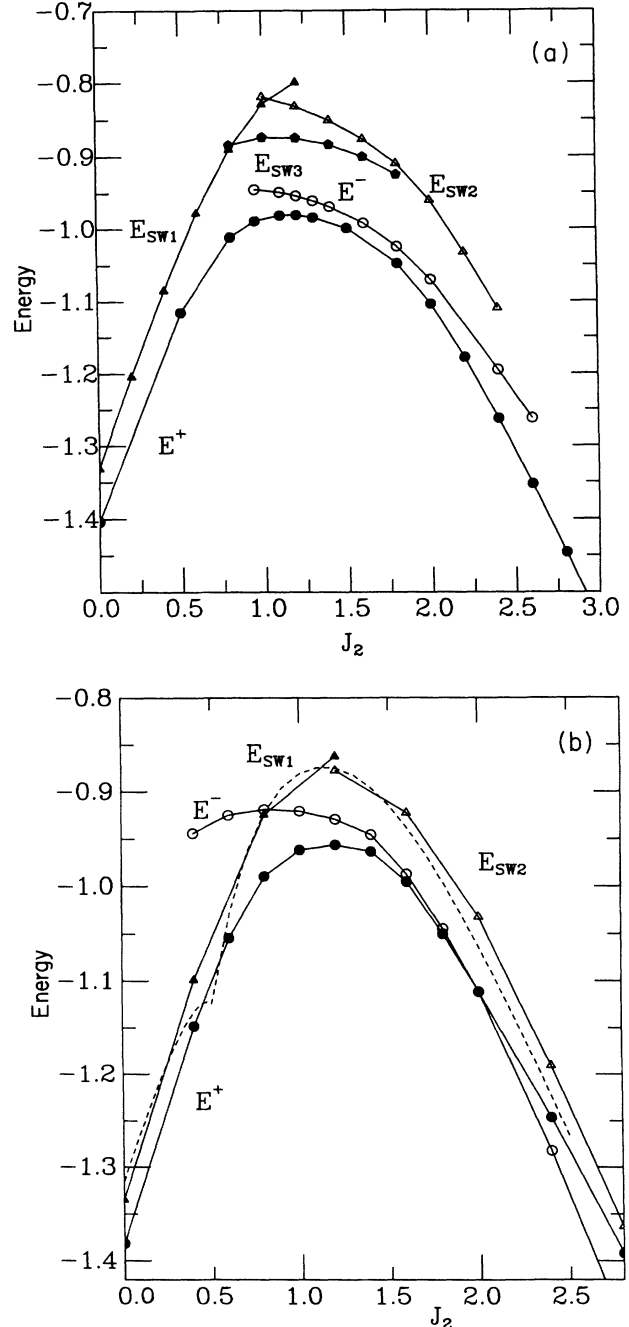


FIG. 5. (a) Ground-state energy of the J_1 - J_2 - J_3 model for ($J_3 = J_2/2$) on a 16 site lattice. E^+ is the ground state, E^- is the first excited state odd under a $\pi/2$ rotation, and $E_{SW1,2,3}$ are spin-waves states as explained in the text. (b) Same as Fig. 5(a) but for the 20 site lattice. Only the spin one states $E_{SW1,2}$ are shown. The dashed line denotes the energy in the spin-wave approximation.

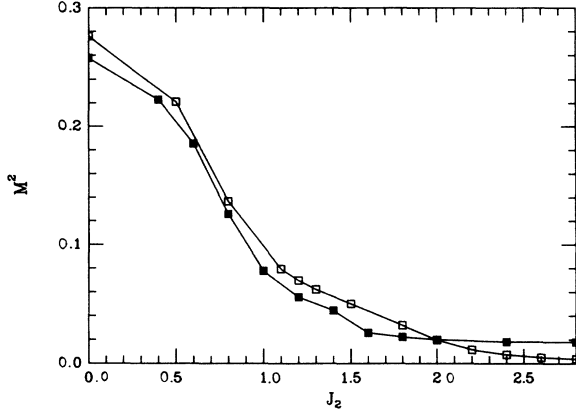


FIG. 6. Staggered magnetization M^2 as a function of J_2 for $J_3 = J_2/2$ and $J_1 = 2$. Solid (open) squares denote results for $N = 20$ (16).

would be that the magnetization in the bulk limit will vanish somewhere between 0.5 and 1.0.

At this point it is convenient to discuss special finite-size effects of this model that may affect the results. There are two important details: (i) for the 4×4 lattice, J_3 couples spins with an effective coupling constant which is doubled from its original value due to the PBC. This may affect the value of the coupling where M^2 becomes a small number, (ii) in the limit of large J_3 working as usual for $J_3 = J_2/2$ our model reduces to the $J_1 - J_2$ model (on two identical sublattices) at exactly the classical critical point $J_2/J_1 = 0.5$. From our results in this model¹² we know that quantum mechanically this point belongs to the region where dimer or twisted order may occur. This limit may easily affect our conclusions for the finite J_3 specially on a small lattice. Also note that for the 20 site lattice in the large J_3 limit the lattice decouples into two $J_1 - J_2$ models on 10 site lattices which cannot accommodate the correct “strip” or collinear order for this model as discussed before in Ref. 12.

In Fig. 7 we show two other squares of order parameters. The twisted susceptibility¹⁷ is given by

$$\chi_t = \left\langle \left[\frac{1}{N} \sum_i [\mathbf{S}_i \times (\mathbf{S}_{i+\hat{x}} + \mathbf{S}_{i+\hat{y}})] \right]^2 \right\rangle. \quad (22)$$

It is clear that χ_t is enhanced in the region where the staggered magnetization (M^2) decreased to a small number. The results for 16 and 20 sites show similar systematic behavior as that of the $J_1 - J_2$ model¹² i.e., χ_t for 20 sites is larger than for 16 sites (although in the present model it occurs on a wider region of parameter space). This is different from the behavior of M^2 and it may be due to finite-size effects³² or differences between the 16 and 20 site lattice that are not clear. Also note that from the definition of χ_t , this susceptibility should remain constant (rather than increasing) with the number of sites if a twisted order is favorable. In any case, the behavior of χ_t shows that the twisted state is strongly enhanced when the Néel state becomes unstable. This state has IC correlations. Actually analyzing $S(\mathbf{q})$ Eq. (2) but now for the

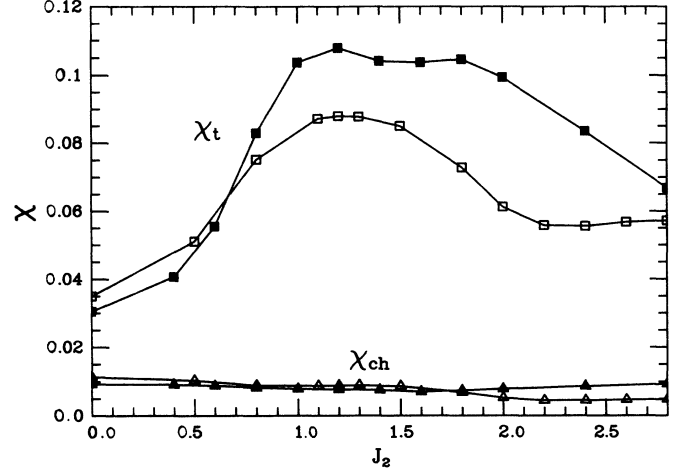


FIG. 7. χ_t (squares) and χ_{ch} (triangles) vs J_2 for $J_3 = J_2/2$ and $J_1 = 2$. Solid (open) squares and triangles denote results for $N = 20$ (16).

spin system [Fig. 8(a) and (b)] we found that the peak at (π, π) in the absence of frustration weakens and actually begins moving after J_2 reaches some value. This is also in excellent agreement with the results of Fig. 5(a) where the lowest-energy spin one state is plotted as a function of J_2 . Note that our results for the 20 site lattice suggest that the peak in $S(\mathbf{q})$ moves towards $(0, \pi)$ or $(\pi, 0)$ rather than $(\pm\pi/2, \pm\pi/2)$. From our small lattice we can not show convincingly that $S(\mathbf{q})$ at other values different from (π, π) will diverge in the thermodynamic limit so the IC correlations may be short range. All these results are very much reminiscent of what we found for the t - J model as a function of doping i.e., IC *short-range* correlations appear when frustration or doping is added into the system. Thus, there seems to exist some qualitative relation between the frustrated Heisenberg model at $J_3 = J_2/2$ and the t - J model.

Note that the spin-wave calculation of the previous subsection showed us that the line we are analyzing corresponds to a disordered phase where the IC order disappeared. However, we are finding that χ_t is strongly enhanced. This may be indicating a deficiency of the spin-wave approach or the presence of a new type of non-classical order.

In Fig. 7 we also show the square of the order parameter corresponding to a *uniform* chiral state defined as

$$\chi_{ch} = \left\langle \left[\frac{1}{N} \sum_i (\mathbf{S}_i \cdot \mathbf{S}_{i+\hat{x}} \times \mathbf{S}_{i+\hat{y}}) \right]^2 \right\rangle. \quad (23)$$

As it happened in the pure $J_1 - J_2$ model¹² the introduction of frustration does not enhance this type of chiral order. χ_{ch} is very flat and never drastically changes its value at $J_2 = 0$. We have also analyzed *staggered* chiral order i.e., we introduced a factor $(-1)^{i_x + i_y}$ in Eq. (22). This is related with the double spiral state of Ref. 13. The result for this susceptibility resembles very much the uniform chiral parameter χ_{ch} i.e., it is flat without showing interesting structure.

Finally, we have also studied the square of the order

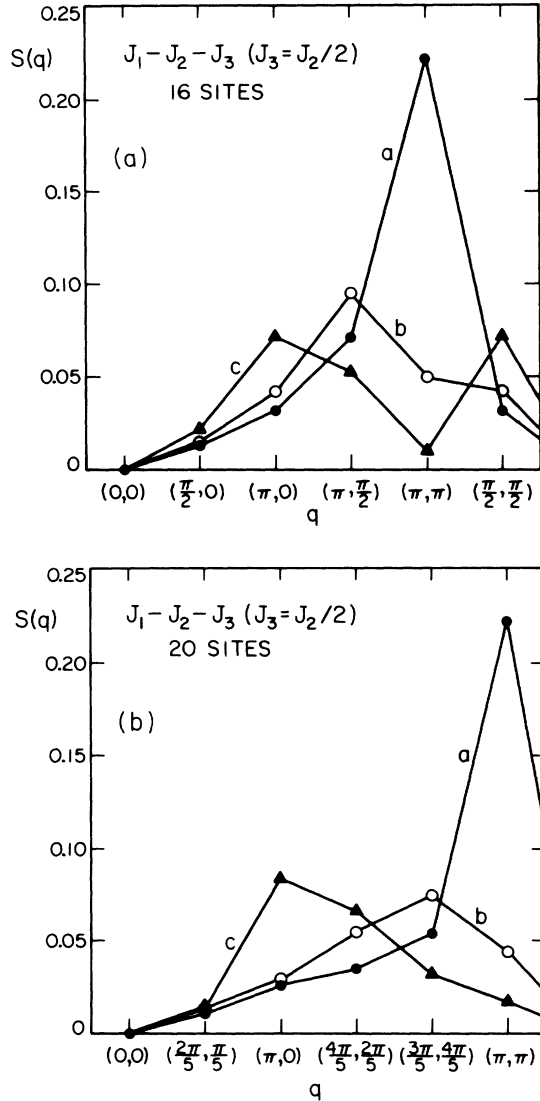


FIG. 8. Spin-spin correlation function $S(q)$ as a function of momentum for the $J_1 - J_2 - J_3$ model on a 16 site lattice (at $J_3 = J_2/2$). (a) denotes results for $J_2 = 0.5$, (b) for $J_2 = 1.5$ and (c) for $J_2 = 2.2$.

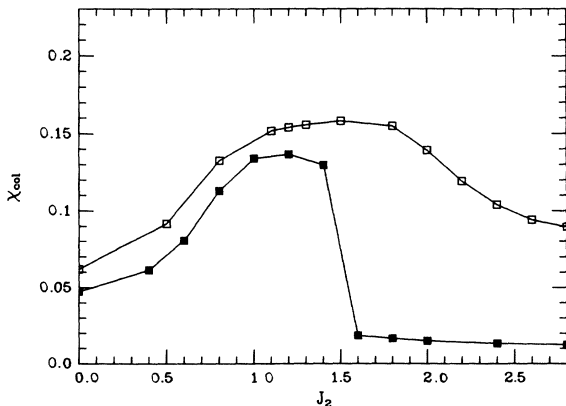


FIG. 9. χ_{col} vs J_2 for $J_3 = J_2/2$ and $J_1 = 2$. Solid (open) squares denote results for $N = 20$ (16).

parameter³⁷ corresponding to a dimer state¹⁶ defined as

$$\chi_{\text{col}} = \left\langle \left[\frac{1}{N} \sum_l \eta(l) \mathbf{S}_l \cdot (\mathbf{S}_{l+\hat{x}} + i\mathbf{S}_{l+\hat{y}} - \mathbf{S}_{l-\hat{x}} - i\mathbf{S}_{l-\hat{y}}) \right]^2 \right\rangle, \quad (24)$$

where l runs only over even sites and $\eta(l) = +1(-1)$ if both l_x and l_y are even (odd). This operator takes the values $1, i, -1, -i$ for the column or dimer state and it vanishes for the Néel state. The results are shown in Fig. 9. Its behavior is very similar to that found for the $J_1 - J_2$ model i.e., the presence of frustration enhances this type of order. χ_{col} is slightly smaller for the 20 site lattice than for the 16 site lattice. Note also from Fig. 9 that there are strong finite-size effects for $J_2 > 1.5$. As remarked above we believe that in that region the decoupling of the 20 sites lattice into two 10 sites sublattices that do not accommodate collinear order may play an important role.

IV. CONCLUSIONS

In this paper we studied the possible existence of incommensurate correlations in the t - J model as a function of doping and in the frustrated spin- $\frac{1}{2}$ model as a function of frustration. For the t - J model we indeed found that adding a certain number of holes (depending on J/t) $S(q)$ shifts the position of its maximum from (π, π) to the closest available momentum on our small lattice. However, when this happens the intensity of the peaks is already greatly reduced and thus we think that the IC correlations are short ranged. Of course, our lattice has small resolution and it may occur that the shift of the antiferromagnetic peak begins as soon as we start doping the system although our results so far suggest that a *finite* doping is necessary for that effect to begin. We have presented a phase diagram of the t - J model in good agreement with a previous mean-field calculation.²⁸ We have not analyzed whether there is a spiral order producing the short-range IC correlations or if domain walls of holes are responsible for this effect but this work is in preparation.

With respect to the frustrated Heisenberg model we found that spin-wave theory predicts narrow regions in the $J_1 - J_2 - J_3$ parameter space where the system may be disordered. In particular one of those regions includes the line $J_3 = J_2/2$. We performed exact diagonalization studies of that line searching for new types of magnetic order in the ground state. We found that after the point where the Néel state becomes unstable, the square of order parameters corresponding to twisted and dimer states presents a maximum. The behavior of these order parameters with the number of sites is as in the previous analysis of the $J_1 - J_2$ model.¹²

From the results obtained from the $J_1 - J_2$ model,¹² the present analysis and new recent results for the triangular lattice with nnn interactions³⁸ we conclude that the uniform chiral state does not seem to be the ground state of spin models with frustration. At least for the

$J_1 - J_2 - J_3$ the same conclusion is reached for the staggered chiral state. That of course does not exclude the possibility that other models may present this type of order. Currently, we are analyzing the presence of chiral order in the t - J model with holes.

ACKNOWLEDGMENTS

We thank P. Chandra, P. Coleman, D. Frenkel, M. Gabay, and E. Siggia for useful comments and E. Rastelli for useful correspondence. This project was supported in part by the National Science Foundation (NSF) Grants Nos. PHY87-01755, PHY82-17853, DMR87-21673 and supplemented by funds from NASA. T. J. is supported by Centre National de la Recherche Scientifique (CNRS). The computer simulation was done mainly on the CRAY-2 at NCSA University of Illinois at Urbana-Champaign and also on the Culler-7 computer at the University of California at Santa Cruz. We thank the National Center for Supercomputing Applications (NCSA) for their support.

APPENDIX

In this appendix we will describe in detail phase 2 of Fig. 4 where the phenomenon of "order from disorder" takes place. To understand this interesting behavior we investigate the $J_1 - J_2$ frustrated model ($J_3 = 0$) beyond $\alpha_2 = \frac{1}{2}$. When J_2 is very large and $S = \infty$ the two sublattices decouple and we have two square lattices with antiferromagnetic coupling. Thus each of them will have as a classical ground state a Néel configuration of spins. It is important to note that the relative angle between the spins of two sublattices is arbitrary. When we add a nearest-neighbor interaction term (J_1) the energy remains independent of the relative angle: the NN bonds

just cancel each other. There is thus a continuum of degenerate classical ground states. Their energy is lower than that of the Néel state as soon as $\alpha_2 > \frac{1}{2}$. We now perform the spin-wave expansion around such a ground state characterized by a relative angle called θ between the directions of the two staggered magnetizations. We will find that the zero-point fluctuations of the spin waves lift the degeneracy in θ and actually there are two states which are true minima with respect to quantum corrections characterized by $\theta = 0, \pi$. This phenomenon has been previously emphasized by many authors^{30,18} in the context of the square-lattice XY model and by Oguchi, Nishimori, and Taguchi in the case of the fcc antiferromagnet.³⁹

At each site i , there is, in general, an angle ϕ_i between the classical orientation of the spin in the ground state and a fiducial quantization axis, say Oz . It is very convenient to express the Hamiltonian in terms of spin operators each quantized in the direction of classical orientation, i.e., at an angle ϕ_i with respect to the original Oz . In terms of local frames, the nearest-neighbor part of the Hamiltonian is rewritten as

$$H_1 = \sum_{\langle ij \rangle} \cos(\phi_i - \phi_j) (S_i^z S_j^z + S_i^x S_j^x) + \sin(\phi_i - \phi_j) (S_i^x S_j^z - S_i^z S_j^x) + S_i^y S_j^y. \quad (\text{A1})$$

For a classical configuration of the spins which is two Néel sublattices with relative angle θ , we note that the horizontal bonds are characterized by the same value of the cosine of the angle θ between the classical directions of the spins and furthermore that the vertical bonds are characterized by the opposite value of the cosine. The nearest-neighbor term can thus be expanded as

$$H_1 = S \sum_h \left[c(b_i^\dagger b_i + b_j^\dagger b_j) - \frac{1+c}{2}(b_i b_j + b_i^\dagger b_j^\dagger) + \frac{1-c}{2}(b_i b_j^\dagger + b_j^\dagger b_i) \right] + S \sum_v \left[-c(b_i^\dagger b_i + b_j^\dagger b_j) - \frac{1-c}{2}(b_i b_j + b_i^\dagger b_j^\dagger) + \frac{1+c}{2}(b_i b_j^\dagger + b_j^\dagger b_i) \right], \quad (\text{A2})$$

where h (v) means that the sum runs over horizontal (vertical) bonds and $c = \cos\theta$. The J_2 term is the simple antiferromagnetic contribution [Eq. (5)] (forgetting the classical energy):

$$H_2 = \alpha_2 S \sum_{nnn} (b_i^\dagger b_i + b_j^\dagger b_j - b_i b_j - b_i^\dagger b_j^\dagger). \quad (\text{A3})$$

After Fourier transforming this expression, one has to diagonalize the quadratic form

$$S \sum_{\mathbf{k}} \left[b_{\mathbf{k}}^\dagger b_{\mathbf{k}} \left[2\alpha_2 + \frac{1+c}{2} \gamma_{\mathbf{k}}^v + \frac{1-c}{2} \gamma_{\mathbf{k}}^h \right] - \frac{1}{2} (b_{\mathbf{k}} b_{-\mathbf{k}} + b_{\mathbf{k}}^\dagger b_{-\mathbf{k}}^\dagger) \left[\frac{1-c}{2} \gamma_{\mathbf{k}}^v + \frac{1+c}{2} \gamma_{\mathbf{k}}^h + 2\alpha_2 \gamma_{\mathbf{k}}' \right] \right], \quad (\text{A4})$$

where $\gamma_{\mathbf{k}}^h = \cos k_x$, $\gamma_{\mathbf{k}}^v = \cos k_y$. The Bogoliubov transformation is now given by

$$\tanh 2\theta_{\mathbf{k}} = \frac{2\alpha_2 \gamma_{\mathbf{k}}' + [(1-c)/2] \gamma_{\mathbf{k}}^v + [(1+c)/2] \gamma_{\mathbf{k}}^h}{2\alpha_2 + [(1+c)/2] \gamma_{\mathbf{k}}^v + [(1-c)/2] \gamma_{\mathbf{k}}^h} \equiv \frac{A_{\mathbf{k}}}{B_{\mathbf{k}}}. \quad (\text{A5})$$

The spin-wave operators are defined as previously by Eq. (12). The staggered magnetization is still given by Eq. (13) and the c -dependent part of the ground-state energy comes from the zero-point contribution

$$E_0(c) = 2S \sum_{\mathbf{k}} \sqrt{B_{\mathbf{k}}^2 - A_{\mathbf{k}}^2}. \quad (\text{A6})$$

This function can be studied numerically since it is perfectly explicit. The minimum energy is reached for $c = \pm 1$ i.e., $\theta = 0, \pi$. There are thus two degenerate states that are selected by quantum fluctuations. They have alternating rows (or columns) of spins up and down (that we will call “strip” or collinear states). Taking $c = 1$ we find for the ground-state energy

$$\frac{E_0}{NJ_1} = -2S(S+2) + 2S \int \frac{d^2k}{(2\pi)^2} [(2\alpha_2 + \cos k_y)^2 - (2\alpha_2 \gamma'_k + \cos k_x)^2]^{1/2}. \quad (\text{A7})$$

Following a similar procedure we have found that along the line $J_3 = J_2/2$ the classical degeneracy [Eq. (15)] is lifted by quantum corrections. On the other hand, on this line the staggered magnetization diverges leading to the conclusion that there is no long-range order. It is not clear how the two phenomena can coexist. Note, however, that the spin-wave approximation even in the absence of long-range order still gives reliable informa-

tion on the energy: this is the case of the spin- $\frac{1}{2}$ chain. Here we can also see [Fig. 5(b)] that the energy of the true ground state is still close to the spin-wave prediction even beyond the point $J_2/J_1 > \frac{1}{4}$. We therefore think that the qualitative phenomenon of “order from disorder” happens beyond that point. It may be related with short-range correlations rather than long-range ones.

*Service de Physique Théorique, Centre d'Etudes Nucleaires de Saclay, F-91191 Gif-sur-Yvette CEDEX, France.

†Departamento de Física, Facultad de Ciencias Exactas, Av. Pellegrini 250, 2000 Rosario, Argentina.

¹J. G. Bednorz and K. A. Müller, *Z. Phys. B* **64**, 188 (1986); C. W. Chu *et al.*, *Phys. Rev. Lett.* **58**, 405 (1987).

²C. Varma, P. Littlewood, S. Schmitt-Rink, E. Abrahams, and A. Ruckenstein, *Phys. Rev. Lett.* **63**, 1996 (1989).

³A. Moreo and E. Dagotto (unpublished); I. Sega and P. Prelovsek (unpublished); C. X. Chen and H. B. Schüttler (unpublished).

⁴T. Thurston *et al.*, *Phys. Rev. B* **40**, 4585 (1989) and references therein. See also G. Shirane *et al.*, *Phys. Rev. Lett.* **59**, 1613 (1987) and R. Birgeneau *et al.*, *Phys. Rev. B* **39**, 2868 (1989).

⁵D. Poilblanc and T. M. Rice, *Phys. Rev. B* **39**, 9749 (1989).

⁶H. Schulz, *Phys. Rev. Lett.* **64**, 1445 (1990).

⁷N. Bickers, D. Scalapino, and S. White, *Phys. Rev. Lett. B* **62**, 961 (1989).

⁸J. Zaanen and O. Gunnarsson, *Phys. Rev. B* **40**, 7391 (1989).

⁹B. Shraiman and E. Siggia, *Phys. Rev. Lett.* **61**, 467 (1988); *ibid.*; **62**, 1564 (1989); *Phys. Rev. B* **40**, 9162 (1989).

¹⁰X. G. Wen, F. Wilczek, and A. Zee, *Phys. Rev. B* **39**, 11413 (1989); V. Kalmeyer and R. Laughlin, *Phys. Rev. Lett.* **59**, 2095 (1988). The chiral operator was studied long ago by Villain, *J. Phys. (Paris)* **38**, 385 (1977) in the context of frustrated spin systems.

¹¹R. Kiefl *et al.* (unpublished).

¹²E. Dagotto and A. Moreo, *Phys. Rev. Lett.* **63**, 2148 (1989).

¹³C. Kane, P. Lee, T. Ng, B. Chakrabarty, and N. Read, *Phys. Rev. B* **41**, 2653 (1990).

¹⁴A. Moreo, D. Scalapino, R. Sugar, S. White, and N. Bickers, *Phys. Rev. B* **41**, 2313 (1990).

¹⁵M. Imada and Y. Hatsugai, *Phys. Soc. Jpn.* **58**, 3752 (1989).

¹⁶N. Read and S. Sachdev, *Phys. Rev. Lett.* **62**, 1694 (1989).

¹⁷P. Chandra, P. Coleman, and A. Larkin, *Phys. Rev. Lett.* **64**, 88 (1990).

¹⁸E. Rastelli, L. Realto, and A. Tassi, *J. Phys. C* **16**, L331 (1983); **19**, L423 (1986); A. Pimpinelli, E. Rastelli, and A. Tassi, *J. Phys. Condens. Matter* **1**, 2131 (1989).

¹⁹M. Gelfand, R. Singh, and D. Huse, *Phys. Rev. B* **40**, 10801 (1989).

²⁰J. Marston and I. Affleck, *Phys. Rev. B* **39**, 11538 (1989).

²¹P. W. Anderson, *Mater. Res. Bull.* **8**, 153 (1973); S. Kivelson, D. Rokhsar, and J. Sethna, *Phys. Rev. B* **35**, 8865 (1987).

²²F. C. Zhang and T. M. Rice, *Phys. Rev.* **37**, 3759 (1988).

²³Actually other more involved terms appear besides this one but in some examples we have shown explicitly that including them in the calculation does not affect the conclusions of this paper.

²⁴E. Dagotto, R. Joynt, A. Moreo, S. Bacci, and E. Dagliano, *Phys. Rev. B* **41**, 2585 (1990); **41**, 9049 (1990).

²⁵Phase separation may also occur in the Hubbard and t - J models for very small J/t , see, e.g., M. V. Feigelman, *Pis'ma Zh. Eksp. Teor. Fiz.* **27**, 491 (1978) [*JETP Lett.* **27**, 462 (1978)]; G. Montambaux, M. Heritier, and P. Lederer, *J. Low Temp. Phys.* **47**, 39 (1982); L. B. Ioffe and A. I. Larkin, *Phys. Rev. B* **37**, 5730 (1988); V. Emery, S. Kivelson, and H. Q. Lin, *Phys. Rev. Lett.* **64**, 475 (1989). For indications of a (small) binding energy of holes on a 4×4 Hubbard model see E. Dagotto, A. Moreo, R. Sugar, and D. Toussaint, *Phys. Rev. B* **41**, 811 (1990).

²⁶Our twisted BC affect the hole hopping term but not the Heisenberg term and is inspired by the Hubbard model. Another way to proceed would have been to write a SU(2)-like twisted BC for the spins.

²⁷A. Kampf and J. R. Schrieffer (unpublished).

²⁸C. Jayaprakash, H. Krishnamurthy, and S. Sarker, *Phys. Rev. B* **40**, 2610 (1989).

²⁹M. Inui, S. Doniach, and M. Gabay, *Phys. Rev. B* **38**, 6631 (1988); J. Annett, R. Martin, A. McMahan, and S. Satpathy, *ibid.* **40**, 2640 (1989).

³⁰J. Villain, R. Bidaux, J. Carton, and R. Conte, *J. Phys. (Paris)* **41**, 1263 (1980); C. Henley, *Phys. Rev. Lett.* **62**, 2056 (1989).

³¹P. Chandra and B. Doucot, *Phys. Rev. B* **38**, 9335 (1988).

³²R. Singh and M. Gelfand (private communication).

³³P. A. Anderson, *Concepts in Solids* (Addison-Wesley, Reading, 1963).

³⁴For the special case $J_2 = 0$ we checked that our results reproduce those of P. Locher, *Phys. Rev.* **41**, 2537 (1990).

³⁵For independent work in this particular line see M. Gabay and P. Hirschfeld (unpublished).

³⁶E. Dagotto and A. Moreo, *Phys. Rev. B* **39**, 4744 (1989); F. Figueirido *et al.* (unpublished).

³⁷S. Sachdev, *Phys. Rev. D* **40**, 5204 (1989).

³⁸T. Jolicoeur, E. Dagotto, E. Dagliano, and S. Bacci, *Phys. Rev. B* **42**, 4800 (1990).

³⁹T. Oguchi, H. Nishimori, and Y. Taguchi, *J. Phys. Soc. Jpn.* **54**, 4494 (1985).